Hindawi Publishing Corporation
X-Ray Optics and Instrumentation
Volume 2010, Article ID 412323, 16 pages
doi:10.1155/2010/412323

Review Article

Thin Shell, Segmented X-Ray Mirrors

R. Petre

X-ray Astrophysics Laboratory, NASA Goddard Space Flight Center, Greenbelt, MD 20771, USA

Correspondence should be addressed to R. Petre, robert.petre-1@nasa.gov

Received 14 May 2010; Accepted 29 November 2010

Academic Editor: Stephen L. O'Dell

Thin foil mirrors were introduced as a means of achieving high throughput in an X-ray astronomical imaging system in applications for which high angular resolution was not necessary. Since their introduction, their high filling factor, modest mass, relative ease of construction, and modest cost have led to their use in numerous X-ray observatories, including the Broad Band X-ray Telescope, ASCA, and Suzaku. The introduction of key innovations, including epoxy replicated surfaces, multilayer coatings, and glass mirror substrates, has led to performance improvements and in their becoming widely used for X-ray astronomical imaging at energies above 10 keV. The use of glass substrates has also led to substantial improvement in angular resolution and thus their incorporation into the NASA concept for the International X-ray Observatory with a planned 3 m diameter aperture. This paper traces the development of foil mirrors from their inception in the 1970s through their current and anticipated future applications.

1. Introduction

The thin foil X-ray mirror was invented to fulfill a particular observational objective. In the 1970's, with the introduction into X-ray astronomy of high resolution imaging through the Wolter I mirrors on the Einstein Observatory, it became recognized that not all applications for which imaging is desired require high angular resolution (<1 arcmin). High angular resolution comes at a cost: mirrors must be accurately figured and held rigidly. These requirements lead to a thick substrate, high mass, and large expense. Since X-ray imaging above ~0.02 keV requires grazing incidence mirrors, the need for thick substrate material leads to inefficient aperture utilization (i.e., low throughput), and thus limited sensitivity. For some astronomical measurements it is desirable to take advantage of the increased sensitivity afforded by imaging but where high throughput is preferred over angular resolution. This is especially true in situations in which the detection of a large number of photons is required to perform the measurement of interest; examples include spectroscopy of relatively isolated sources and polarimetry. For such applications, replacing a small number of thick, massive, expensive mirror shells with a large number of thin, low mass, low cost shells offers the desired improvement in throughput with sufficient angular resolution to resolve most sources. Thus the driving idea behind the foil mirror was to provide a low cost, low mass, high throughput alternative to high-resolution mirrors.

Since its inception, the foil mirror has shown itself to be versatile and adaptable to a wide range of applications. It has become the starting point for virtually all applications requiring low cost, lightweight mirrors, with moderate imaging applications. Because of its efficient aperture utilization, it has evolved into the baseline design of choice for imaging above 10 keV. Important innovations have been introduced, most importantly the substitution of glass for aluminum foil as the mirror segment substrate. Over time, as demand has increased for improved angular resolution, the design has undergone steady improvement. The principles leading to its invention are the basis for its most ambitious manifestation, the mirror for the International X-Ray Observatory (IXO).

This paper traces the development of the foil mirror. It describes the innovations that have led to its evolution from a simple light bucket to a high-resolution imaging system with applications across a broad energy band.

It should be noted that the many conceptual and implementation innovations leading to the first foil mirrors

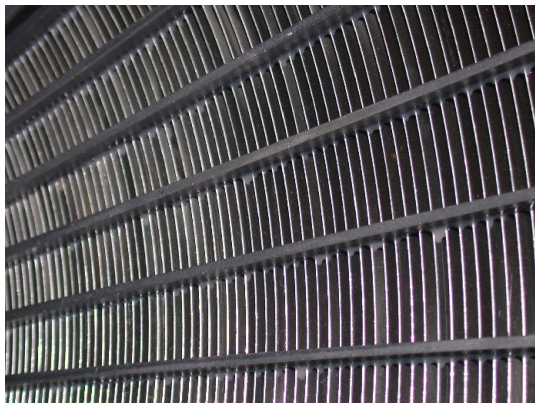

Figure 1: Close-up view of entrance aperture of a foil mirror. The large number of nested shells plus the use of thin foil substrates combine to provide a large filling factor. The average distance between foils is approximately 1 mm.

were due to Peter Serlemitsos at NASA's Goddard Space Flight Center (GSFC). Not only has he pioneered the concept [1], but he is also responsible for many of the improvements over the past 30 years. He has also led the team that constructed every such mirror that has flown in space thus far. While others are responsible for recent parallel developments towards higher angular resolution (e.g., introduction of glass as a substrate material), it is the work of Serlemitsos that made this type of mirror viable. His contribution to astrophysics through the invention of the thin foil mirror was recognized by his being awarded the 2009 Joseph Weber prize by the American Astronomical Society.

2. Basic Principles

The basic design and principles of the conical foil mirror are described in Serlemitsos [2] and Petre and Serlemitsos [3]. In its pure form, the thin foil mirror is a Wolter I design in which many thin shells are nested to fill the available aperture. A high filling factor (ratio of usable to total aperture) is obtained when the substrate thickness is small compared with the gap between adjacent shells (in contrast to the thick substrates in the high resolution imaging mirrors to date, such as Einstein, ROSAT, and Chandra). Since emphasis is on low cost and high collecting area rather than image quality, the paraboloidal and hyperboloidal surfaces are approximated by conic frusta, thus the term "conical approximation." For large focal ratios (focal length to aperture diameter), the conical approximation introduces only an intrinsic blur of a few to a few tens of arc seconds, depending on the axial length of the mirror segment. The degree of simplification offered by introducing this approximation far outweighs the reduced intrinsic imaging performance, which in actual implementations tends to be small compared with the overall mirror angular resolution.

The optical design of foil mirrors follows a common template (see, e.g., [3]). The mirror shells are nested to maximize the on-axis effective area (Figure 1). This is accomplished by leaving no radial gap between the outer diameter of the front of one shell and the rear of the next shell outward: viewing from the front of the mirror on axis, the entire aperture is covered by either a reflecting surface or the front edge of one. This maximum filling approach leads to a linear off-axis vignetting function. The vignetting with off-axis angle is a function of incident energy, steeper at higher energy. A practical approximation of the diameter of the field of view is given by the average graze angle of the mirror. At radii beyond half the graze angle, the effective area is typically less than half the on-axis area. The angular resolution, if characterized by half power diameter (HPD), is essentially constant across the field of view: off-axis aberrations are small compared with the blur introduced by the conical approximation within the field of view of a typical focal plane instrument. The image of a point source changes from circularly symmetric to elongated perpendicular to the off-axis shift direction, however. Outside the nominal field of view, aberrations (particularly coma and oblique spherical aberrations) degrade the HPD.

The conical design has several practical attributes that simplify construction. First, it can be shown by simple geometric arguments that all the many nested mirror surfaces in each of the two reflection stages (paraboloid analog, usually referred to as the primary surface and hyperboloid analog, referred to as the secondary), when flattened onto a plane, all describe a segment of the same annulus. This means that the substrates can be mass produced, with only two cutting fixtures needed to shape substrates. Second, since no axial curvature is imparted to the reflecting surfaces, surface preparation can be kept simple (e.g., forming the overall shape of a relatively smooth substrate). The only requirement on the preparation technique is that it produces or preserves a surface that is smooth on spatial scales larger than approximately 1 mm. Various coating techniques can then provide the necessary smoothness on smaller spatial scales. Third, the design lends itself to modularity and mass production. The mirror is usually divided into angular segments, quadrants, or thirds, with a separate housing for each.

The introduction of the conical approximation greatly reduces the precision requirements on the substrate. A number of substrate materials have been tried, but the best-suited material is aluminum. Aluminum has low density, the right balance between stiffness, and ductility to allow forming and can be found in large, thin rolls or sheets with high gloss finish.

The method used for shaping aluminum into the conical form has changed minimally since its first use. If the raw stock comes from a roll, it was first flattened by compression between two glass plates under heat. The aluminum is cut approximately to shape and then given its basic shape (a segment of a cone frustum) by pressing it against a mandrel and thermally cycling it. The aluminum is formed so that global surface structure such as roll marks runs along the direction of incidence of the radiation to minimize scatter off surface features that remain after coating. (This means that stock from a roll needs to be flattened so that curvature can be introduced in the opposite direction.) Refinements in this process include the mandrel shape (originally cylindrical,

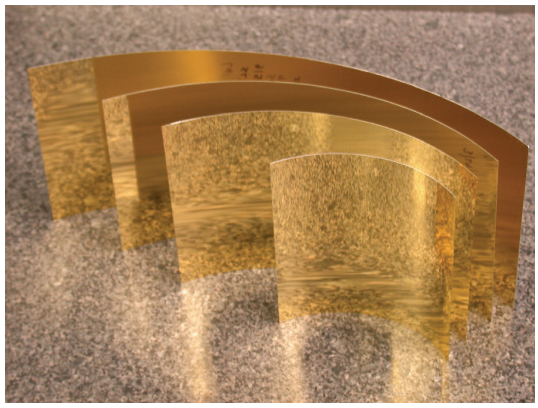

Figure 2: Finished foil mirror segments. These particular mirror segments were produced using epoxy replication, but appear identical to those produced using lacquer coating.

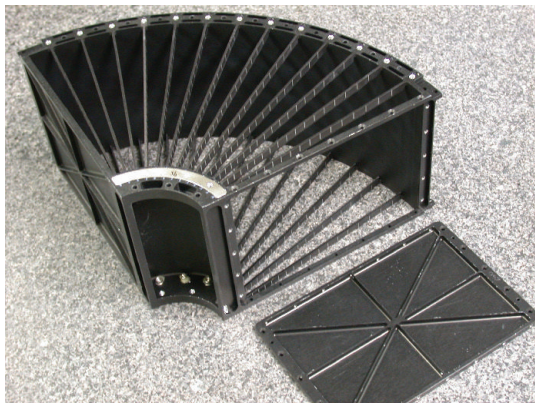

(a)

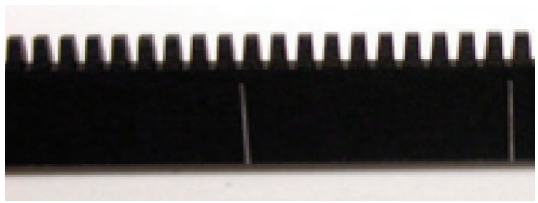

(b)

Figure 3: (a) Assembled conical mirror quadrant housing. Two such housings (primary and secondary) are stacked to form a complete quadrant. Mirror segments are inserted from the open side through the grooves in the radial alignment bars. (b) Magnified view of a portion of an alignment bar. The width at the base of the angled grooves is slightly larger than the segment thickness.

now conical, and with increasing radial accuracy), how the substrates are held against mandrels (originally mechanically and now using suction), and the details of the thermal cycle used for the forming.

Even aluminum sheet stock with the most mirror-like appearance has a surface structure making it an inefficient X-ray reflector. It tends to have unacceptably high roughness on spatial scales shorter than a few millimeters, which if not removed would introduce unacceptably high scattering of incident X-rays. Additionally, the X-ray reflecting surface needs to be coated with a high-density metal (e.g., Ni or Au) to obtain high X-ray reflectivity.

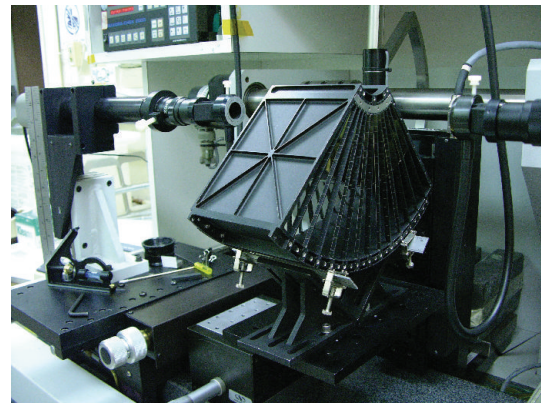

Figure 4: One reflection stage of a mirror quadrant being undergoing alignment on an optical table. Microscopes (left and right) view the edges of the mirror segments as the housing is rotated about the mirror optical axis, allowing them to be accurately positioned.

The initial solution to the roughness problem and the one that made foil mirrors a viable technology was the use of acrylic lacquer [2]. It was found that immersing the shaped aluminum segments in a lacquer bath and slowly drawing them out left a thin, uniform, microscopically smooth surface coating. An X-ray reflective surface was applied via evaporation of a thin layer of gold (Figure 2). This was the approach used for the first conical mirrors.

Another important aspect of the foil mirror concept is modularity [2]. A complete shell is divided into equal arc lengths, initially quadrants. This eases manufacture of substrates and handling of both substrates and modules.

Mounting in a housing and aligning 100 or more pairs of mirror segments is challenging, and misalignment remains a primary source of blur. Serlemitsos [2] introduced gang alignment, whereby all of the segments in the primary or secondary housing are loaded together and are held in place front and rear by a set of accurately grooved radial alignment bars. Substantial research has gone into optimizing the number of alignment bars as well as the shape of the grooves. The grooves must be precisely located and not allow the segments to shift. At the same time they cannot be so narrow as to prevent insertion of segments or to distort them. A housing and a magnified portion of an alignment bar are shown in Figure 3.

Gang alignment offers the substantial benefit that it can be done relatively quickly (Figure 4). Its primary disadvantage is the limit it places on angular resolution—aligning all the segments to the best average focus introduces segment-to-segment variation. The need for the grooves to be wider than the segments to allow loading without damaging the segments and introducing distortions leads to the introduction of a small variation in mirror slope, in turn leading to blur. This slope error tends to be random within a quadrant and is typically an arc minute in the mirrors developed for flight.

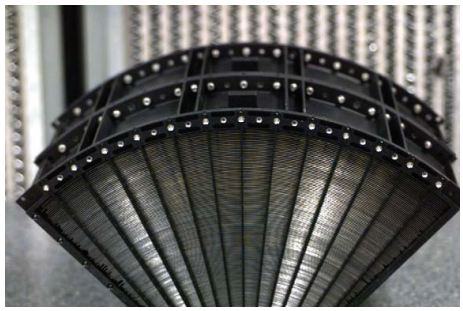

Figure 5: A completed quadrant, viewed from the front.

Primary to secondary alignment is generally performed in an optical beam, while the location of the focus and quality of the image is monitored. Figure 5 shows a completed module, in this instance a quadrant. Once all the modules comprising a mirror (primary plus secondary) have been populated and internally aligned, they are mounted on a ring. Alignment at this stage entails only shifting the foci of the respective modules via translation; since each module separately acts as a thin lens, small overall tilts can be ignored. The net effect of a slight tilt is the reduction of the on-axis effective area.

3. The First Foil Mirrors

A total of eight flight quality lacquer coated foil mirrors were produced at GSFC between 1987 and 1992. The parameters of these mirrors are summarized in Table 1. One of these was for a sounding rocket instrument, two for the Broad Band X-ray Telescope (BBXRT), and five for the Japan/US X-ray observatory ASCA (four flight plus one spare). The properties of these mirrors are listed in Table 1.

The first conical mirror to fly was constructed in 1987 for a Supernova X-ray Spectrometer sounding rocket payload, intended to search for X-ray emission from SN 1987A [2]. The mirror was adopted from the (not yet built) BBXRT design, but the focal length was reduced from 3.84 m to 2.1 m. It was launched in February 1988 with a pixilated Si(Li) detector at its focus. During its five-minute exposure above the atmosphere, it detected LMC X-1 as well as hot, diffuse emission from the LMC, but not SN 1987A, which it failed to observe due to an attitude control program error. The mirror was recovered intact. Its primary success was a demonstration that such mirrors can survive a launch environment and deliver the expected performance in space. This mirror has recently been renovated and will be used on the Micro-X sounding rocket instrument [4].

The first real application of a foil mirror was BBXRT. The objective of this instrument was to perform sensitive, moderate resolution spectroscopy of a variety of X-ray sources over the 0.3–12.0 keV band. This band contains the K line radiation of all astrophysically abundant metals (O, Ne, Mg, Si, S, Ca, Ar, Fe), plus the L lines of iron. This instrument carried a pair of coaligned foil mirrors, each illuminating a pixilated Si(Li) detector. The mirrors have a 40 cm diameter and focal length of 3.84 m; each was constructed of 118 nested shells, constructed in quadrants. The axial length of each reflection stage was 10 cm. The mirror segments were produced by lacquer coating 0.127 mm thick aluminum foil substrate and overcoating the lacquer with gold for X-ray reflection. Each mirror had a mass of 20 kg. BBXRT was flown in December 1990 for nine days as part of the Astro-1 payload on Shuttle mission STS-35, performing approximately 150 observations of 85 celestial targets. The performance of the instrument, including the mirrors, is described in detail in Weaver et al. [5].

The broadband point spread function was determined on orbit by comparing the distribution of counts from discrete cosmic sources with models based on ground calibration. It was best modeled using a pair of Gaussian profiles. The inner image core ($\sigma = 1.8$ arcmin) contained 65 percent of the source flux; the outer halo ($\sigma = 5.8$ arcmin) contained 35 percent. Some energy dependence of the point-spread function was observed; this was ascribed to residual roughness of the mirror foils. The degree of energy dependence was not quantified, but consistent with that measured for the mirrors on ASCA, which were fabricated using the same approach (see below). The effective area of each mirror was approximately 290 cm^2 at 1 keV and 125 cm^2 at 7 keV.

The Japanese-US ASCA was the first free flying, general use X-ray observatory to incorporate foil mirrors [6]. With its foil mirrors and its groundbreaking CCD detectors, ASCA made numerous important contributions to astrophysics and demonstrated the utility of both high throughput mirrors and CCD detectors.

ASCA was severely mass limited, with a total mass of ~400 kg. Thus there was a premium on the effective area-to-mass ratio of the X-ray mirrors, a situation for which foil mirrors provide the best solution. ASCA incorporated four identical coaligned foil mirrors, each with a mass of 10 kg [7]. Two mirrors illuminated imaging gas scintillation proportional counters, the other two illuminated the first CCD detectors ever used in an orbiting X-ray observatory. Each mirror had a diameter of 35 cm and a 3.5 m focal length and consisted of 120 nested shells. The foil thickness and axial length were the same as in BBXRT. Also as in BBXRT, the mirror surfaces were produced using the lacquer coating, with an evaporated gold overcoat. One of the flight mirrors is shown in Figure 6.

ASCA was launched on February 20, 1993, and operated in orbit for six years. The point-spread function had two distinct components, a sharp core plus a halo. While the full width at half maximum was ~1 arcmin, the HPD was 3.6 arcmin. While the HPD was largely constant across the 0.5–10 keV energy band, the halo did show some energy-dependent broadening. This is ascribed to small angular scale roughness on the mirror surfaces. The fractional flux in the broadened component varied from 8 percent at 1.5 keV to 17 percent at 8 keV. The broadening is consistent with the measured surface microroughness of ~3 Å. Despite the modest dimensions and mass of the mirrors, each of the four had an effective area of approximately 300 cm^2 at 1 keV and 140 cm^2 at 8 keV. There was no appreciable difference among the four mirrors. Over the six-year mission life, no degradation of the mirror performance was observed.

Table 1: Foil mirror parameters.

	SXS/Micro-X	BBXRT	SODART	ASCA	Astro-E/E2 SXT-I	Astro-E/E2 SXT-S
Number flown	1	2	0	4	8	2
Diameter (cm)	40	40	60	35	40	40
Focal length (m)	2.1	3.77	8	3.5	4.75	4.5
Number of Shells	68	118	143	120	175	168
Number of modules per mirror	4	4	4	4	4	4
Segment length (cm)	10	10	20	10	10	10
Total number of segments	544	944	1144	960	1400	1344
AI Substrate thickness (mm)	0.127	0.127	0.4	0.127	0.152	0.152
Surface production method	lacquer	lacquer	lacquer	lacquer	replication	replication
Reflective coating	gold	gold	gold	gold	gold	gold
Mass (kg)	20	20	101	9.84	19.3	19.9
Effective area at 1 keV (cm^2)	300	290	950	300	450	450
Effective area at 7 keV (cm^2)	—	125	750	150	250	250
Angular resolution (HPD-arcmin)	3	3	2.4–3.8	3.6	1.6-1.7	1.7
Year of launch	1988	1990	—	1993	2000, 2005	2000, 2005

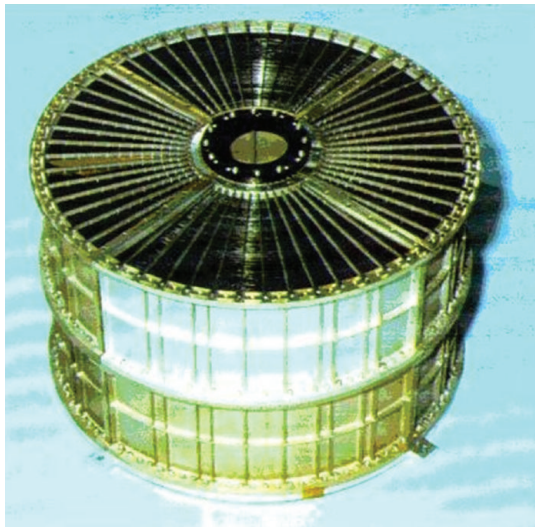

Figure 6: An ASCA flight mirror, one of five constructed. The aperture diameter is 35 cm; the height is approximately 20 cm. The mirror consists of 118 nested shells and has a mass of 10 kg.

The most ambitious application of lacquer-coated mirrors was the pair constructed for the SODART, Soviet-Danish Röntgen Telescope [8]. The SODART instrument was to have flown in the 1990s on the Russian Spectrum X-Gamma observatory, but the observatory was never launched. Each of the two mirrors had a 60 cm diameter and an 8 m focal length. It consisted of 143 nested shells divided into quadrants like the GSFC mirrors. The shells were thicker (and thus stiffer) than those used at GSFC (0.4 mm as opposed to 0.127 mm) and longer (20 cm as opposed to 10 cm). The mirror forming and mounting approaches largely duplicated those used at GSFC for BBXRT and ASCA [9]. One exception is that the segments were bonded to the housing sides after alignment of a primary and secondary quadrant. The reflecting surfaces were prepared using a similar lacquer coating technique to that developed at GSFC. Each mirror weighed 101 kg.

Extensive ground testing was performed on the SODART mirrors [10]. The measured performance was strongly dependent on the field of view of the detector, the result of large angle scattering off surface imperfections. The half power diameter ranged from 2.4 arcmin to 3.8 arcmin, depending on field of view and energy. The on-axis effective area was 765 cm^2 at 6.6 keV and was 65 percent of that expected from an ideal geometry, independent of energy.

4. Epoxy Surface Replication

One attribute of the lacquer-coated mirrors was the presence of "orange peel" on their surfaces—millimeter-scale ripples that limited their angular resolution. This surface roughness was a major source of blur and is likely to be largely responsible for the field of view and energy dependence of the angular resolution best quantified for the SODART mirrors, but common to all lacquer-coated mirrors. The quest to remove this effect led to the introduction of epoxy replication [11]. Epoxy replication is a proven technique for producing optical components. It is a standard way for instance of making gratings. For X-ray astronomy, epoxy was used to produce the mirrors for ESA's Exosat mission [12] and the reflection gratings on the XMM-Newton mission [13]. If epoxy replication was to work for thin foil mirrors without sacrifice of their reasonable cost, then it was necessary to develop a straightforward process that would consistently produce better quality mirror surfaces than lacquer coating and lend itself to mass production.

The replication process introduced by Serlemitsos and Soong [11] does just that. First, the thin reflective layer (gold or platinum) is deposited onto a glass mandrel. Then a thin,

even layer of epoxy is sprayed onto the preformed aluminum substrate and/or the coated mandrel. The mandrel and substrate are brought into contact under vacuum and then brought to atmosphere to force the two together. The epoxy is allowed to cure in air for several hours at an elevated temperature. Once the epoxy is cured, then the mirror segment is separated from the mandrel. The segment is trimmed to its final shape for installation into its housing; the mandrel is cleaned in preparation for another replication cycle.

A number of factors contribute to the success of this approach. Inexpensive, durable mandrel material needed to be found. Drawn cylindrical borosilicate glass tubing manufactured by Schott has a surface with very low microroughness that is transferred to the epoxy. Mandrels are selected by scanning the surface of a tube to find portions with minimal curvature (typically less than 1 arcmin). The smooth microsurface of the mandrels allows the deposited reflective layer to release easily, with no need for a release layer. Additionally, since the reflective layer is deposited onto the mandrel, it is possible to use sputtering instead of evaporation. Sputtering yields a layer with density closer to bulk than evaporation and thus a higher X-ray reflectivity (the gold on the ASCA and BBXRT mirrors had density ~85 percent of bulk). For the replication to be viable, it was essential to find an epoxy that could be thinned to allow uniform spraying of a thin layer. A spraying process then needed to be developed that yields a uniform coating (this was done via robotic spraying—see Figure 7). Using a sufficiently thin epoxy layer minimizes transfer of large-scale mandrel surface features onto the substrate, meaning that the substrates retain the shape imparted to them through heat forming. The thin epoxy layer is also necessary to minimize distortions due to stresses built up during curing, as well as bilayer thermal deformation. Finally an epoxy cure cycle was developed that was not too cool, lest the epoxy cure insufficiently, nor too hot, lest the epoxy intermix with the reflecting material and spoil the surface quality.

5. Epoxy-Replicated Flight Mirrors: Astro-E and Suzaku (Astro-E2)

Epoxy replication has become the baseline approach for making foil mirrors. The first epoxy-replicated mirrors were built for the Japan/US Astro-E mission. Included in the Astro-E instrumentation were five 40 cm diameter epoxy-replicated foil mirrors [14]. Four mirrors illuminated CCD detectors, which together comprise the XIS instrument. These mirrors had a focal length of 4.75 m and consisted of 175 nested shells. The fifth mirror illuminated an X-ray microcalorimeter: a unique, nondispersive imaging spectrometer with high spectral resolution, that operates at a temperature of 0.065 K. This mirror had a 4.5 m focal length and consisted of 168 shells. The reflection stages of both mirror types again had an axial length of 10 cm. Each mirror had a mass of approximately 19 kg; the reflectors comprised over half the total mass.

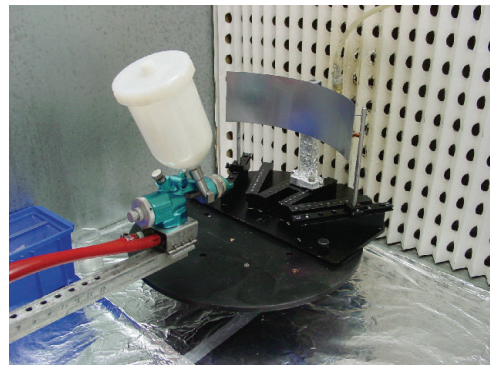

Figure 7: Epoxy coating of a foil using a robotic sprayer.

The Astro-E mirrors underwent extensive ground calibration in a pencil beam facility [15]. The HPD was found to be 1.8–2.2 arcmin for the five mirrors and was largely energy independent in the 1.5–8.0 keV range. This represents a substantial improvement over the resolution obtained by the lacquer-coated ASCA mirrors. The effective area of each mirror was 20 percent lower than the design values at all energies. Analysis of this loss ascribed 11 percent to mechanical misalignment and slope errors of the mirror segments, 6 percent to reflector surface roughness (5.1 Å rms), and 3 percent to wide-angle scattering of radiation beyond the boundary of the focal plane detector. Nevertheless the effective area of each mirror was ~450 cm^2 at 1 keV and ~250 cm^2 at 7 keV, a high throughput for such a modest diameter mirror.

Astro-E was launched on February 10, 2000. A first stage booster failure prevented the spacecraft from reaching orbit. To recover from this setback, a nearly identical Astro-E2 spacecraft was built. The foil mirrors are largely identical in design and construction to those of Astro-E [16]. The single major change was the addition of a stray light baffle, which was attached to the front of each mirror to largely eliminate the paths to the focal plane of radiation reflected only off the secondary reflector [17]. Additionally, a more restrictive screening was applied to the glass tubes used as replication mandrels in order to reduce the figure error of the mirror segments. Extensive ground calibration was performed using a pencil beam [18]; one of the five mirrors was calibrated using full illumination [19]. The minor process improvements yielded a slightly improved angular resolution over that of the Astro-E mirrors: the HPD was 1.6–1.7 arcmin. The effective area was essentially identical to that of the Astro-E mirrors. The same 20 percent reduction in effective area below the design area as for the Astro-E mirrors was found. It was shown that the loss of effective area due to misalignment between the mirror and the stray light baffle was at most 2 percent. A finished flight mirror is shown in Figure 8.

Astro-E2 was successfully launched on July 10, 2005, and renamed Suzaku upon reaching orbit. Because of the loss of cryogen from the microcalorimeter cryostat prior to the start of observations, only the mirrors illuminating the CCD detectors were calibrated in orbit. The in-flight effective

Figure 8: An Astro-E2 flight mirror, with stray light baffle attached on top. The aperture diameter is 40 cm; the height is approximately 22 cm. The mirror consists of 168 nested shells and has a mass of 20 kg. Between Astro-E and Astro-E2 (Suzaku) a total of 10 such mirrors were constructed.

area was found to be consistent with ground calibration. A slight degradation of the angular resolution was noted immediately after launch: the on-orbit HPD of the four mirrors is 1.8–2.3 arcmin. The reduction is thought to be the consequence of mechanical relaxation of the foil segments in their housings stimulated by launch vibrations (the segments are not bonded in place). Over nearly five years since launch there has been no detectable change in the performance of the mirrors.

6. Future Foil Mirrors: The Astro-H Soft X-ray Telescope, GEMS, and Astrosat

Astro-H is the next major Japan/US X-ray observatory, currently under development in Japan for a 2014 launch. Its instrumentation includes four X-ray mirrors: two Soft X-ray Telescopes (SXTs) for imaging in the 0.3–10 keV band and two Hard X-ray Telescopes (HXTs) for imaging in the 10–50 keV band. All are foil mirrors. One of the SXTs will illuminate a microcalorimeter detector, the other a CCD detector. The HXTs are described below; the key parameters of both are listed in Table 2

The SXT design is a scaled up and improved version of Suzaku's [20]. The mirror has a 45 cm diameter and a 5.6 m focal length. As with Suzaku and the other foil mirrors, the SXT is constructed in quadrants. The segment length will again be 10 cm. The total number of nested shells is 203. The required angular resolution is 1.7 arcmin HPD. The expected effective area of the mirror will be about 510 cm^2 at 1 keV and 390 cm^2 at 7 keV. An exploded view of the mechanical design is shown in Figure 9. Most of the components shown in this figure are common to all foil mirrors.

Several process improvements are being incorporated into the SXT fabrication process in order to improve the angular resolution, toward achieving 1.3 arcmin HPD or better [20].

(i) Closer attention is being paid to the shape of the substrates. More accurate forming mandrels are being fabricated. Fewer mirror substrates will be stacked onto a forming mandrel during each forming run. This reduces figure errors introduced by forcing a segment into a radius for which it has an incorrect cone angle.

(ii) Three different substrate thicknesses are being used: 0.125, 0.229, and 0.305 mm, with thicker substrates at larger radii. The use of thicker, thus stiffer, substrates should yield mirrors with final shape closer to the ideal one.

(iii) A thinner epoxy layer will be used ($\sim 12\,\mu$m versus $\sim 25\,\mu$m on Suzaku). There is a mismatch between the conical shape of the raw substrate material and the cylindrical replication mandrels. Use of a thicker, stiffer epoxy layer, which conforms to the shape of the replication mandrel, therefore introduces stresses on the substrate and can deform it. Use of the thinner layer will allow replication of the very smooth mandrel surface, but allow the substrate to retain the shape imposed upon it during forming.

(iv) A modified alignment and mounting scheme will be used, incorporating two distinct sets of radial bars. One set of reference bars, with precisely located and shaped grooves, will be used as in the past to perform gang alignment of the mirror segments. A second set of support bars, with larger grooves, will be interspersed with the reference bars, and the aligned segments will be bonded to them. After bonding, the accurate reference bars will be removed; only the second set will fly. Experiments using this approach on groups of 40–80 segments indicate improvement of the HPD to ≤ 1.2 arcmin.

(v) The mirror has a substantially higher mass allowance (44 kg, compared with the 20 kg per Suzaku mirror). While the total mass of the mirror substrates is considerably larger than Suzaku (due to both the larger number of substrates and the use of thicker aluminum), the housing will comprise a larger fraction of the mirror mass (41 percent, compared with 25 percent for Suzaku). The resulting stiffer housing will reduce blur.

Foil mirrors also are being utilized on the Gravity and Extreme Magnetism Small Explorer (GEMS), a mission devoted to X-ray polarimetry scheduled for a 2014 launch. GEMS has three identical telescopes, each consisting of a foil mirror and a novel, time projection chamber X-ray polarimeter. The instrument operates in the 2–10 keV band. While the polarimeter is not an imaging instrument, use of an imaging mirror allows accurate placement of a concentrated beam at its small entrance aperture, thus substantially increasing instrument sensitivity. The mirror design is based on the Suzaku design, with the same 4.5 m focal length. Fitting three coaligned telescopes in the SMEX fairing constrains the diameter of each mirror to be 32 cm.

Table 2: The foil mirrors being developed for Astro-H.

	SXT	HXT
Diameter (cm)	45	45
Focal length (m)	5.6	12
Number of shells	203	213
Number of modules per mirror	4	3
Segment length (cm)	10	20
Total number of segments	1624	1278
AI Substrate thickness (mm)	0.152, 0.229, 0.305 mm	0.2 mm
Surface production method	replication	replication
Reflective coating	gold	Pt/C multilayer
Mass (kg)	56	80
Effective Area (cm^2)	510 @ 1 keV	800 @ 6 keV
	390 @ 7 keV	200 @ 40 keV
Angular resolution (arcmin)	1.7 (goal <1.3)	2 (goal <1. 7)

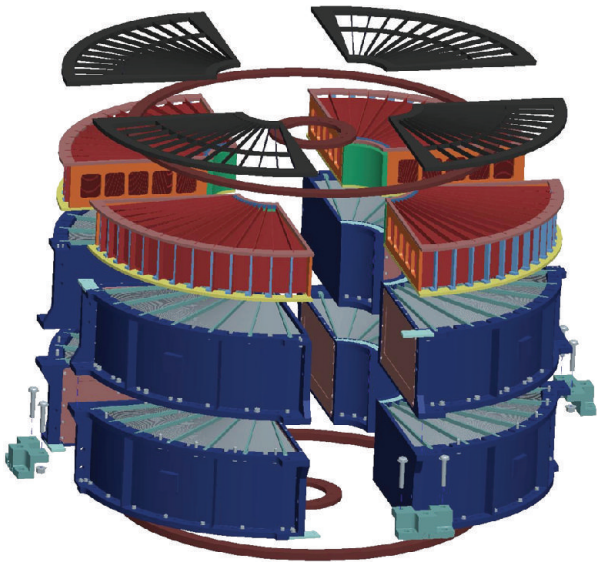

Figure 9: Exploded view of the Astro-H Soft X-ray Telescope. The mirror is segmented into quadrants. The main components, from the bottom, are inner and outer lower mounting rings, the two reflection stages, the stray light baffle, the inner and outer upper mounting rings, and the thermal shield. The overall dimensions of the assembled mirror are 47 cm in diameter and 25 cm high.

The GEMS mirrors are thus basically a smaller diameter version of the Suzaku mirrors, with 110 nested shells. The same forming and replication mandrels will be used to produce the segments, and the same lightweight housing design will be used, scaled to the smaller diameter. The resulting difference in effective area from the Suzaku mirrors primarily affects the band below 2 keV where the detectors are not sensitive. The angular resolution requirement is 1.3 arcmin, better than that achieved on Suzaku, but achievable given the smaller size and number of shells and taking advantage of some of the process improvements developed for Astro-H. Each mirror will have a mass of 10 kg.

The Indian observatory Astrosat, to be launched around 2012, will include in its instrumentation a modest X-ray imaging system consisting of a foil mirror and a CCD detector [21]. The mirror will have a focal length of 2.0 m and a diameter of 26 cm. The angular resolution is estimated to be about 3 arcmin. The effective area will be about 200 cm^2 at 2 keV and 25 cm^2 at 6 keV. The mirror segments will be fabricated using the same replication process as for Astro-E/E2 and subsequent foil mirrors. The mirror is being constructed at the Tata Institute of Fundamental Research, where the facility used for constructing the Astro-E/E2 mirrors was duplicated.

7. Multilayers

Imaging in the hard X-ray band, above 10 keV, is a true experimental challenge. Because the fluxes of all cosmic X-ray sources decline with increasing energy, performing detailed imaging observations requires substantial collecting area. At the same time, the critical angle of even the highest density metallic coatings becomes very small, leading to very large focal ratio mirrors. (Typically, for a given coating, the maximum energy that can be imaged $E_{\max}$ is proportional to the ratio of the focal length F to the mirror diameter d: $E_{\max} \propto F/d$.) However, shorter focal ratios that can realistically be implemented into instruments can be obtained by the use of multilayer coatings.

A multilayer consists of alternating layers of high and low Z material, with typical bilayer thicknesses of a few nm. The thickness of the two layers is controlled during deposition to produce efficient Bragg scattering at reasonable grazing angles for energies of interest. A uniform multilayer has efficient response only over a narrow range of energies. The invention of graded multilayers has made possible mirrors with a broadband response [22]. The layers have increasing thickness according to some prescription as a function of distance from the substrate. The thicker, outer layers reflect X-rays from the lower end of the band of interest, while the higher energy X-rays that penetrate more deeply into the layer are reflected by the deeper, more closely spaced layers. The original concept for graded multilayers introduced a power law layer variation with distance. Yamashita et al. [23] introduced the "supermirror" concept wherein the continuous gradation is replaced by a series of groups of identical thickness layers. They showed that the X-ray reflectivity of such a multilayer is comparable to that expected from an optimum grading.

Foil mirrors are attractive as high-energy mirrors because of their large geometric filling factor. With multilayers applied to the surfaces, they become efficient mirrors above 10 keV. Table 3 lists segmented multilayer mirrors that have either flown or are under construction.

The initial means for applying multilayers onto substrates was to coat the multilayers on top of the gold surface of an epoxy replicated segment [23]. This is an inherently slow and low yield approach because of the great

Table 3: Multilayer coated foil mirrors.

	InFOCμS	HEFT	SUMIT	NuSTAR
Diameter (cm)	40	24	36	38
Focal length (m)	8	6	8	10
Number of shells	255	72	90	130
Number of modules per mirror	4	1*	3	1*
Segment length (cm)	10	2×10**	13	22.5
Total number of segments	2040	700	540	2340
Substrate material	aluminum	glass	aluminum	glass
Substrate thickness (mm)	0.17	0.3	0.22	0.21
Surface production method	replication	thermal forming	replication	thermal forming
Multilayer coating	Pt/C	W/Si	Pt/C	Pt/C, W/Si
Effective area (cm^2)	51	50@40		150
Angular resolution (arcmin)	2.7	1.3	2.06	<60
Year of launch	2001, 2004	2005	2006	2012

*HEFT and NuSTAR mirrors consist of one module, but shells are composed of multiple segments.
**Each reflecting stage consists of a pair of segments.

care that must be taken to not damage the epoxy surface by overheating during deposition (the epoxy surfaces will be damaged if heated about ~40°C). It was subsequently demonstrated that multilayers could be replicated the same way as a gold monolayer: the multilayer is grown on a glass mandrel and then transferred to the aluminum substrate using epoxy replication. This introduced a major advance in production speed and yield.

This approach was used to produce the first multilayer imaging mirror for hard X-rays [24, 25]. This mirror was used on the International Focusing Optics for MicroCrab Sensitivity (InFOCμS) balloon instrument, flown for the first time in 2001 (and an upgraded version flown twice subsequently), and has produced the first images of cosmic sources in the 20–40 keV band using multilayers. This mirror used the same fabrication, mounting, and alignment techniques as used for Astro-E/E2, the only difference being the use of replicated multilayers for the reflecting surface instead of a gold monolayer. Like the Astro-E mirrors, it has a diameter of 40 cm, but it has a focal length of 8 m. A total of 255 nested shells are required. A graded Pt/C multilayer was transferred via epoxy replication onto each substrate. In the most recent mirror upgrade, the substrates were divided into 12 groups by radius, with the same multilayer prescription applied to each substrate in a group [26]. The block prescription introduced by Yamashita et al. [23] was used to determine the number of layers and the thickness of each [27]. Each mirror segment had between 28 and 78 layers, with layer thickness between 2.61 nm and 12.64 nm. This mirror has an angular resolution of 2.1–2.4 arcmin in the 20–60 keV band and an effective area of 51 cm^2 at 30 keV [28].

A mirror of similar design was constructed using the InFOCμS approach for the Supermirror Imaging Telescope (SUMIT) balloon instrument [29, 30]. Design differences were introduced in order to improve the angular resolution and the effective area (through the reduction of misalignments). The key differences were the use of thicker and longer foils (to increase stiffness and reduce the number), subdividing shells into thirds rather than quadrants (to reduce end effects), and using single housing unit instead of separate modules (to increase overall structural stiffness). These changes did lead to improved angular resolution and effective area over InFOCμS. The angular resolution measured on the ground was 2.06 arcmin. Despite the fact that only the inner 36 cm of the 40 cm aperture was populated with segments, the effective area at 30 keV was virtually the same as the 40 cm diameter InFOCμS mirror. This indicates that coupled with the higher angular resolution, less light was lost due to misalignment or internal blockage. SUMIT was launched from Brazil in late 2006, but unfortunately was lost at sea.

The combined experience of the InFOCμS and SUMIT mirrors has been employed in the design of the Hard X-ray Telescopes (HXTs) that will fly on Astro-H [31]. These mirrors are being constructed by a consortium of Japanese institutions led by Nagoya University. The HXTs are the most ambitious hard X-ray mirrors under development. Each has a diameter of 45 cm and a 12 m focal length. As was the case for SUMIT, each shell is divided azimuthally into only three segments, and an integral housing is used. The mirror consists of 213 nested shells. Aluminum substrates 0.2 mm thick will be used. The mirror segments are 20 cm long in order to reduce the number of nested shells and increase the clear aperture. Another innovation is that the housings will be considerably more massive, to minimize distortions. Each mirror has a total mass of 80 kg, four times more massive than the Suzaku mirrors. The required angular resolution is 2 arcmin (HPD), but the expected angular resolution is <1.7 arcmin. Graded Pt/C multilayers, designed using the supermirror approach, are transferred to the segments. The expected effective area of each mirror is 800 cm^2 at 6 keV and 420 cm^2 at 40 keV.

8. Limiting Factors to Angular Resolution in Foil Mirrors

Over the 30 years of development, there has been substantial improvement in foil mirror performance. The angular resolution has improved incrementally with each new generation of mirror. The introduction of epoxy replication removed the energy dependence of the point-spread function. More accurately machined and stiffer housings have reduced misalignments. Better substrates and forming mandrels have reduced figure errors on individual segments. Nevertheless, no foil mirror has attained an angular resolution better than one arc minute.

A number of error budget analyses for various foil mirror implementations have been presented (e.g., [30–32]). The key contributors to blur include misalignment of segments within the housing, misalignment of primary and secondary segments, macroscopic axial figure errors on the foil surfaces, and distortions introduced by the mismatch between the segment shape and its location in the housing (effectively delta-delta-R errors). The intrinsic angular resolution due to the conical approximation is generally small compared with any of these terms. These analyses universally conclude that several terms contribute approximately equally. Thus all must be addressed if significant improvement is to be achieved. From the discussion above about the Astro-H SXT design, it can been seen both that incremental improvements are still being made and, more importantly, that addressing errors across a broad front can potentially lead to a considerably better mirror. Still it is unlikely that an aluminum foil mirror will ever achieve angular resolution substantially better than one arc minute. As we describe below, however, use of a different substrate material allows for construction of a high angular resolution mirror that preserves many of the desirable attributes of the foil mirror.

9. Glass as a Substrate

Aluminum has numerous desirable attributes as a substrate material for foil mirrors: low density, easy to form, moderate cost, good surface properties. Nevertheless it is not ideal; it is flimsy, cannot be formed in three dimensions (i.e., cannot impart the axial curvature of a true Wolter mirror), and most importantly the surface quality of even the best material limits the attainable resolution to about an arc minute, considerably worse than the intrinsic resolution of the conical approximation for typical designs. Hailey et al. [33] performed a careful characterization of the surface properties of Al and concluded that the surface properties limit the angular resolution of even a perfectly aligned aluminum foil mirror to 25 arcsec. Hailey was especially interested in a substrate to which multilayers could be applied. For a W/Si multilayer, Mao et al. [34] found that the interfacial roughness on glass (3.5–4.0 Å) was lower than that on an epoxy replicated foil (4.5–5.0 Å) (they did not try multilayer replication).

A number of alternative materials have been proposed: different metallic foil, silicon, carbon fiber-reinforced plastic. Each of these materials introduces a new set of challenges. The most promising alternative material, and one that has produced a revolution in thin substrate mirrors, is glass. In searching for an alternative substrate for aluminum for hard X-ray mirror for a balloon instrument, Hailey et al. [33] showed that the intrinsic surface quality of commercially available borosilicate glass is far superior to that of aluminum. Moreover, the glass he investigated, commercially available Schott Desag D263 and AF45, has good mechanical properties, even at thicknesses of 200–400 μm. Hailey developed a thermal slumping approach to form the glass to its approximate shape. Multilayers could be directly deposited onto the glass substrate without a microroughness increase.

The slumping approach introduced by Hailey et al. [33] entails suspending a flat piece of glass substrate across a concave mandrel, and slowly thermally cycling it so that the glass assumes the form of the mandrel. While the figure of the substrate is not precise (Hailey et al. use cylindrical molds), the excellent microroughness of the surface is preserved. A slow thermal cycle in which the glass is annealed as it cools allows the glass to largely retain its mechanical properties.

The first use of glass substrates in a full mirror was for the High Energy Focusing Telescope, a balloon instrument led by CalTech with mirrors supplied by Columbia University. HEFT was designed to be sensitive in the 20–70 keV band. The mirror surfaces were therefore coated with a graded multilayer, in this case composed of tungsten and silicon. The mirror consists of 70 shells, with an outer diameter of 24 cm and a 6 m focal length. Each shell was conical approximation of a Wolter 1 and was comprised of 20 elements. The primary and secondary each consisted of two 10 cm long, end-to-end sets of five azimuthal segments. Each segment was 0.2 mm thick.

The HEFT mirror introduced a novel mounting and alignment scheme. The mirror was built outward from a central core. A set of carbon spacers was attached to the existing outermost shell (or the central core). The outer surfaces of these spacers were then machined in situ to the proper diameter and slope for the next shell. Then the 20 glass segments comprising the next shell were epoxied to the spacers, while the image formed by the shell was monitored optically. Once the epoxy set, the next layer was attached the same way. This mounting scheme is illustrated in Figure 10 and the mounting fixture in Figure 11. This mounting approach has three significant advantages over the approach used for foil segments. Mechanically it yields a rigid structure, which is unlikely to experience changes due to vibration or shock. The in situ machining eliminates stack up error and ensures confocality. The forcing of the stiff glass substrates into contact with the accurately machined spacers forces them to maintain a conical shape to high accuracy. The performance of a mirror constructed using this approach therefore has the potential for better angular resolution than foil mirrors mounted in the traditional way, with the blur dominated by substrate misalignments and figure errors.

Three HEFT mirrors were constructed. Two are shown in Figure 12. The angular resolution of the best mirror was ~1.3 arcmin at 8 keV [35, 36]. There was a clear angular

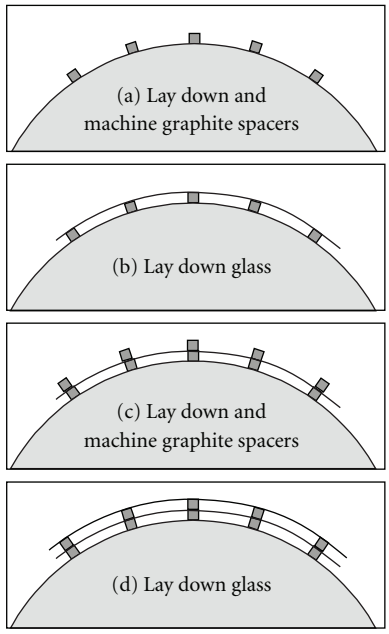

Figure 10: The mounting scheme for thermally formed glass mirrors invented for HEFT.

resolution improvement from the inner shells to the middle ones, across the boundary where the spacer density doubled. This is likely due to the fact that the larger number of spacers forces the glass substrates to conform more closely to the ideal conical surface. The effective area was within 20 percent of expectations from modeling, approximately 20 cm^2 at 25 keV. HEFT was flown in May 2005, but no report of its performance has been published.

10. Future Application of Glass Substrates: NuSTAR

The HEFT balloon mirror serves as the prototype of the Nuclear Spectroscopy Telescope Array (NuSTAR), a Small Explorer expected to be launched in 2012. NuSTAR features a pair of conical slumped glass mirrors. Each mirror has a 38 cm diameter and a 10 m focal length. It consists of 133 nested glass shells with segment length of 22.5 cm. The outer 65 shells consist of 12 pairs of azimuthal segments, the inner 65 of 6 pairs. The angular resolution requirement is 60 arcsec (HPD); the goal is 40 arcsec. Each mirror is expected to have a mass of 24.5 kilograms [37].

The mirror substrates are 210 μm thick D263 glass. They are heat formed into a cylindrical shape. In contrast to the substrates for HEFT, these are thermally formed using convex mandrels incorporating slumping technique developed for IXO (described below). The mandrels are polished commercial grade fused silica. Adopting the approach under development for IXO has resulted in formed glass substrates with excellent figure: the typical two-reflection HPD for the uncoated substrates is 40 arcsec, with many around 30 arcsec. Thus the possibility exists that the integrated mirrors will attain the angular resolution goal.

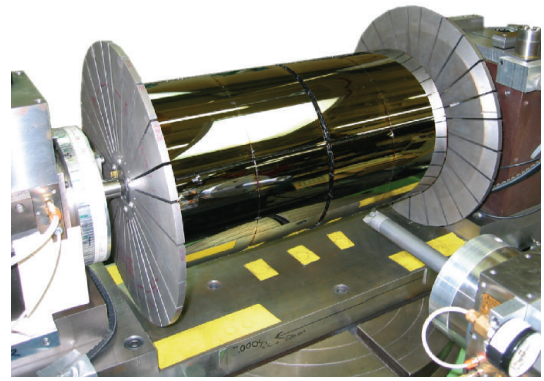

Figure 11: Fixture used to align and mount HEFT.

Figure 12: Two HEFT mirrors. Each mirror is 24 cm in diameter and 40 cm long and consists of 70 nested formed glass shells.

The mirrors are mounted and aligned using the approach developed for HEFT. Improved alignment machines have been fabricated.

11. Slumped Glass Mirrors for Constellation-X/XEUS/IXO

The introduction of slumped glass substrates stimulated work by a number of investigators seeking a means of forming thin substrates capable of providing high angular resolution. The motivation for this work comes from the consensus need for the next major X-ray astronomy mission—a substantial increase in collecting area combined with high angular resolution, to facilitate spatially resolved spectroscopy of distant (and hence faint) objects. The high angular resolution is driven by the need to perform spatially resolved spectroscopy of extended objects (clusters of galaxies, supernova remnants) as well as measure the spectrum of extremely faint objects without source confusion. The original NASA implementation was Constellation-X; the ESA implementation was the X-ray Evolving Universe Spectroscopy (XEUS). In 2007, these missions were merged into the International X-ray Observatory (IXO). For Constellation-X, the baseline implementation utilized slumped glass, with technology development led by GSFC. For XEUS, the baseline mirror was a Silicon Pore Optic

(SPO). Slumped glass was considered a backup technology for XEUS, with technology development at the Max Planck Institut für Extraterrestrische Physik (MPE) and at the *Osservatorio Astronomico di Brera* (OAB). All three institutions are participating in the glass technology development for IXO.

The fundamental differences between Constellation-X and XEUS on one hand, and IXO on the other, are the size and performance specifications of the mirror. Constellation-X incorporated an array of four identical mirrors, each with a 1.3 m diameter and a 10 m focal length. The angular resolution was to be 15 arcsec HPD, with a goal of 5 arcsec. XEUS was to have a single mirror, with 5 m^2 of collecting area and a 50 m focal length. The angular resolution was to be 5 arcsec HPD, with a goal of 2 arcsec. IXO incorporates a single, large diameter mirror with 20 m focal length, 3.3 m diameter, and mass of 1750 kg. The effective area at 1.25 keV is to be at least 2.5 m^2 with a 3.0 m^2 goal and 0.6 m^2 at 6 keV. The angular resolution of the entire observatory is to be 5 arcsec; to achieve this, the mirror angular resolution must be ~3-4 arcsec. Two approaches to the mirror are being pursued. ESA is developing a mirror based on silicon pore optics (SPO), wherein commercially available 0.773 mm thick Si wafers are stacked to form a conical approximation of a Wolter I mirror [38–40]. Careful stacking and alignment of the wafers lead to a mirror in which the dominant component of the angular resolution error budget is the conical approximation. The second approach, under study by NASA and independently in Europe at MPE and OAB, uses segmented glass substrates, slumped into a Wolter shape, and mounted accurately into groups of identical modules [41–43]. Note that unlike previous implementations in which a conical approximation sufficed, true Wolter surfaces are required if the angular resolution requirement is to be met for IXO. But as for previous foil mirrors, a key design parameter in the IXO design is the effective area per unit mass.

A possible slumped glass design for the IXO mirror (Figure 13) consists of 361 nested Wolter I shells [44]. The mirror is divided into three rings of modules. The intent of the modular design is that all the precision alignment and mounting (and thus all technology development) are contained within a module; aligning the modules to each other is straightforward. The inner ring has 12 identical modules, and the middle and outer rings each have 24. Each mirror segment is 20 cm in axial length; no segment has an arc length longer than 40 cm. The inner module contains 143 segment pairs, the middle 115, and the outer 103. Thus a total of 13,986 segments are incorporated into the full mirror. The module structure must be carefully CTE matched to the glass to minimize the introduction of blur due to thermal gradients. The modules vary in mass between 16 and 23 kg.

Thin slumped glass is the substrate of choice because of its combination of desirable mechanical and optical properties. The fundamental technical challenges associated with using slumped glass are (i) how to introduce via thermal forming a surface with a contribution of <1.5 arcsec to the angular resolution error budget; (ii) how to mount and align these flimsy substrates without introducing stresses

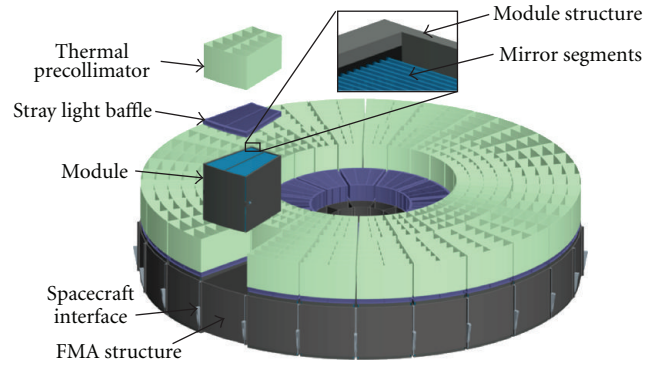

Figure 13: Schematic of the NASA reference design of the IXO mirror. The mirror consists of 361 nested shells, in 60 modules. The overall diameter of the aperture is 3.3 m.

or distortions. While neither goal has been accomplished, substantial progress has been made towards them.

In the NASA approach, the glass is slumped onto a convex mandrel (the European glass mirror development partly retains concave mandrels). The primary reason for using a convex mandrel is because in a concave mold, thickness variations in the substrate, even if they are fractions of a micron, would introduce figure errors even in a substrate that conforms exactly to the mold. In the IXO design, a 1 μm error in the mirror curvature corresponds to a blur of 8 arcsec. Mandrels and formed substrates are shown in Figure 14.

Use of a convex mold means that the X-ray reflecting surface comes into contact with the mandrel. The Columbia group used concave mandrels to avoid this contact, to ensure preservation of the excellent microroughness of the raw material. Zhang et al. have found that use of a suitable release layer on a convex mold preserves the microsurface quality [41]. The microroughness degradation is measured to be a most 1 Å. The challenges faced in forming precise mirror segments are threefold. (i) Mandrels with sufficiently high quality figure need to be mass produced. (ii) Distortions introduced into the glass from the slumping must be controlled. The most destructive distortions are those with spatial frequencies in the millimeter to centimeter range, the so-called midfrequency errors. (iii) Any X-ray reflective coating deposited onto the substrate must not distort it via bimorphic stresses.

Of the three challenges, the most formidable is the control of the midfrequency errors. Several optics manufacturers have the capability for producing mandrels of the required quality and quantity. Experiments have demonstrated that the bimorphic stresses imparted by iridium, the reflective coating of choice, can be compensated by the use of an undercoating material (such as chromium) that imparts opposite stress,. Control of the midfrequency errors depends on the release layer surface quality. Current experiments are concentrated on a boron nitride coating. Once the coating is applied, it must be conditioned through a series of buffing and thermal cycling steps.

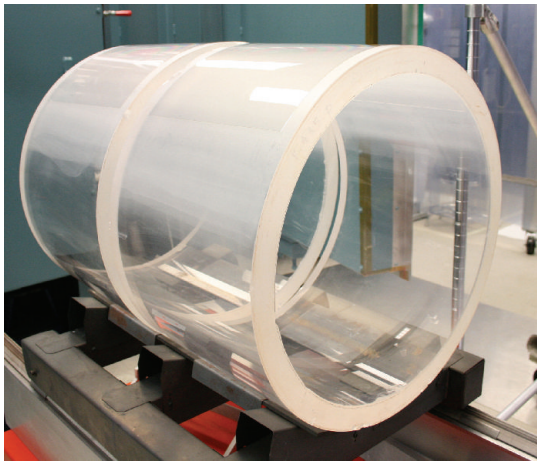

(a)

(b)

Figure 14: Two views of thermally formed glass substrates for IXO on mandrels. The mandrels are fused silica; each is approximately 50 cm in diameter. The two mandrels shown represent the primary and secondary reflection stages for a particular shell.

Results to date are promising. It has been shown that the formed substrates conform to the mandrel figure with very high fidelity. For a number of reasons, the required figure quality has not yet been attained. In order for the full mirror to have 3 arcsec resolution, the error budget requires each segment to have figure errors less than 2.3 arcsec. This is subdivided into error ascribed to the forming mandrel (1.5 arcsec) and error due to the forming process of 1.7 arcsec; dominating this 1.7 arcsec is the midfrequency error due to the release layer. Mandrels with the required 1.5 arcsec HPD are only now available. Individual segments with figure of ~5 arcsec have been fabricated, and refinement of the process could make the requirement reachable within a few months.

The coated substrates must next be mounted accurately in a module without distorting the optical figure. Bending moments applied at mounting points propagate across the entire substrate, compromising the figure. What makes the mounting extremely challenging is that the substrates are

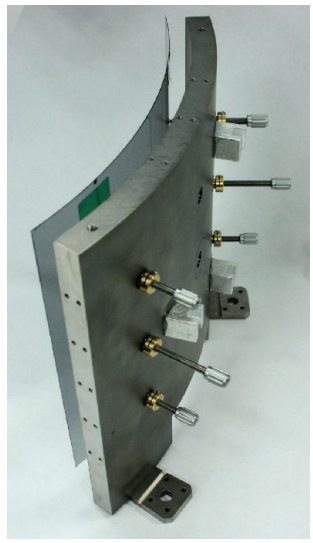

(a)

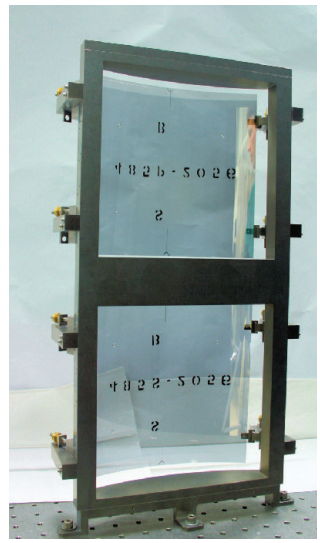

(b)

Figure 15: (a) Rear view of an IXO mirror on a strongback for transfer to a permanent mount. The six actuators provide the mounting points. (b) A pair of uncoated IXO mirror segments mounted in a prototype permanent mount.

flimsy, bending under their own weight. At the same time, alignment tolerances are a fraction of a micron. To accurately align and mount the substrates, they need to be rigidized, but in such a way that the intrinsic shape is preserved. Alternatively, advantage can be taken of the segments' flimsiness, and the capability for correcting first-order figure errors (like out of roundness or cone angle variations with azimuth) can be incorporated into the alignment scheme. Both approaches are under study and are referred to as the "passive" and "active" approaches, respectively.

In the passive approach, the first step is to mount and bond the mirror segment temporarily onto a strongback, converting the flexible mirror segment into a *de facto* rigid body that can be handled, characterized, transported, and aligned (Figure 15). The mirror segment is next located and aligned properly in position and orientation using precision stages under the monitoring of an optical beam with grazing incidence Hartmann tests (i.e., sequential illumination of small angular portions of the mirror pair). Once the segment is aligned, it is bonded at several locations permanently to the module housing structure. The bonding process must not introduce stress or displace the segment. After the permanent bonds have cured, the transfer mount is removed.

In the active approach, radial displacements produced by actuators at the mirror segments' forward and aft ends are used to correct the mirror segments' tilt errors (pitch and yaw) and adjust cone angle to minimize the alignment aberrations of focus error and coma. After achieving the best possible focus, the mirror segment is permanently bonded to the module housing structure. After the permanent bonds have cured, the actuators are disengaged and removed.

X-ray measurements using a single mirror pair were most recently performed in 2007, using a different mounting

approach. The measured HPD was ~15 arcsec, consistent with performance predictions based on optical metrology of the mirror surfaces and the accuracy of the alignment [45]. Since that measurement, both mounting approaches have been shown to produce higher accuracy alignment, and the quality of the mirror segments has improved substantially [41].

Yet another approach would be slumped segments containing both the parabolic and hyperbolic surfaces on a single piece. The feasibility of doing this has been demonstrated at MPE [42]. Although mandrel fabrication for this approach is more challenging, the complexity of aligning the primary and secondary surfaces is avoided, and alignment errors thereby reduced.

12. The Future of Segmented Mirrors

The evolution of thin, segmented X-ray mirrors since their introduction 30 years ago has been remarkable. No longer are they merely considered as concentrators for enhancement of focal instrument sensitivity (although they still play that role on, e.g., GEMS). Through the introduction of new surface deposition methods (multilayers) and substrates (glass), they have evolved into the mirror of choice for high energy imaging (NuSTAR, the Astro-H HXT, and the hard X-ray capability on IXO). With the introduction of accurate substrate forming and precision mounting, they also now have the potential to provide high angular resolution. At the same time, their key advantages—high filling factor, low mass per unit collecting area, suitability for mass production, to name a few—remain attractive features of the design. With two upcoming space missions using (aluminum) foil mirrors (Astro-H and GEMS) and one using glass (NuSTAR), segmented X-ray mirrors play an essential role in the near-term future of X-ray astronomy. Owing to these factors and their scalability to large areas, segmented optics have become the de facto baseline for future X-ray missions.

One realm segmented mirrors opens to future exploration is imaging in very hard X-rays. New material combinations and manufacturing capabilities for multilayer coatings promise to extend the energy band accessible with direct imaging well beyond 100 keV for reasonable focal lengths (10–15 m) [46, 47]. A telescope using such multilayers would be able to detect astrophysically important nuclear transitions such as ^{56}Ni at 158 keV and ^{57}Co at 122 and 136 keV.

As discussed above, the proposed NASA implementation of IXO, which carries X-ray astronomy well into the 2020's, relies on segmented glass. Beyond that, NASA's vision mission Generation-X (Gen-X) calls for a single focal plane mirror system with 50 m^2 at 1 keV, which is unattainable unless a segmented approach is implemented [48]. It also calls for extremely high angular resolution (0.1 arcsec HPD). The starting point toward achieving such high resolution is a successful IXO development program leading to a ~3 arcsec HPD mirror. The angular resolution of this mirror would be further improved by making the mirror surfaces active, through, for example coating the back side of each glass segment with thin-film pixilated electrodes over a thin layer of piezoelectric material and then applying voltage to improve a segment's figure [49]. Segmented X-ray mirrors will continue to play a key role in X-ray astronomy instrumentation for the foreseeable future.

References

[1] P. J. Serlemitsos, "The Broad-Band X-Ray Telescope," in *X-ray Astronomy in the 1980's*, S. S. Holt, Ed., NASA TM 83848, 1981.

[2] P. J. Serlemitsos, "Conical foil x-ray mirrors: performance and projections," *Applied Optics*, vol. 27, no. 8, pp. 1447–1452, 1988.

[3] R. Petre and P. J. Serlemitsos, "Conical imaging mirrors for high-speed X-ray telescopes," *Applied Optics*, vol. 24, no. 12, pp. 1833–1843, 1985.

[4] E. Figueroa-Feliciano, P. Wikus, J. S. Adams et al., "Progress on the Micro-X rocket payload," in *Space Telescopes and Instrumentation 2008: Ultraviolet to Gamma Ray*, vol. 7011 of *Proceedings of SPIE*, June 2008.

[5] K. A. Weaver, K. A. Arnaud, E. A. Boldt et al., "Calibrating the broad band X-Ray telescope," *Astrophysical Journal, Supplement Series*, vol. 96, no. 1, pp. 303–324, 1995.

[6] Y. Tanaka, H. Inoue, and S. S. Holt, "The X-ray astronomy satellite ASCA," *Publications of the Astronomical Society of Japan*, vol. 46, no. 3, pp. L37–L41, 1994.

[7] P. J. Serlemitsos et al., "The X-ray telescope on board ASCA," *Publications of the Astronomical Society of Japan*, vol. 47, no. 1, pp. 105–114, 1995.

[8] H. W. Schnopper, "SODART telescopes on the Spectrum X-Gamma (SRG) and their complement of instruments," in *Advances in Multilayer and Grazing Incidence X-Ray/EUV/FUV Optics*, Proceedings of SPIE, pp. 412–423, July 1994.

[9] J. Polny, N. J. Westergaard, F. E. Christensen, H. U. N. Nielsen, and H. W. Schnopper, "Production, assembly and alignment of the XSPECT mirror modules for the SODART X-ray telescope on the spectrum röntgen gamma satellite," in *Grazing Incidence and Multilayer X-Ray Optical Systems*, vol. 3113 of *Proceedings of SPIE*, pp. 349–359, July 1997.

[10] F. E. Christensen, B. Madsen, A. Hornstrup et al., "X-ray calibration of the SODART flight telescopes," in *Grazing Incidence and Multilayer X-Ray Optical Systems*, vol. 3113 of *Proceedings of SPIE*, pp. 294–306, July 1997.

[11] P. J. Serlemitsos and Y. Soong, "Foil X-ray mirrors," *Astrophysics and Space Science*, vol. 239, no. 2, pp. 177–196, 1996.

[12] R. Laine, R. Giralt, R. Zobl, P. A. J. de Korte, and J. A. M. Bleeker, "X-ray imaging telescope on EXOSAT," in *Space Opt, Imaging X-Ray Opt Workshop*, vol. 184 of *Proceedings of SPIE*, pp. 181–188, 1979.

[13] A. Rasmussen, J. Cottam, T. Decker et al., "Performance characterization of the reflection grating arrays (RGA) for the RGS experiment aboard XMM," in *X-Ray Optics, Instruments, and Missions*, Proceeding of SPIE, pp. 327–337, July 1998.

[14] H. Kunieda, M. Ishida, T. Endo et al., "X-ray telescope onboard Astro-E: optical design and fabrication of thin foil mirrors," *Applied Optics*, vol. 40, no. 4, pp. 553–564, 2001.

[15] R. Shibata, M. Ishida, H. Kunieda et al., "X-ray telescope onboard Astro-E. II. Ground-based x-ray characterization," *Applied Optics*, vol. 40, no. 22, pp. 3762–3783, 2001.

[16] P. J. Serlemitsos, Y. Soong, K. W. Chan et al., "The X-ray telescope onboard Suzaku," *Publications of the Astronomical Society of Japan*, vol. 59, no. 1, pp. S9–S21, 2007.

[17] H. Mori, R. Iizuka, R. Shibata et al., "Pre-collimator of the astro-E2 X-Ray telescopes for stray-light reduction," *Publications of the Astronomical Society of Japan*, vol. 57, no. 1, pp. 245–257, 2005.

[18] K. Misaki, H. Kunieda, Y. Maeda et al., "Ground-based X-ray calibration of the telescopes onboard Astro-E2 satellite," in *Optics for EUV, X-Ray, and Gamma-Ray Astronomy*, Proceedings of SPIE, pp. 294–305, August 2003.

[19] K. Itoh, H. Kunieda, Y. Maeda et al., "Ground-based X-ray calibration of the Astro-E2 X-ray telescope II. With diverging beam at PANTER," in *UV and Gamma-Ray Space Telescope Systems*, Proceedings of SPIE, pp. 85–92, June 2004.

[20] T. Okajima, P. J. Serlemitsos, Y. Soong et al., "Soft x-ray mirrors onboard the NeXT satellite," in *Space Telescopes and Instrumentation 2008: Ultraviolet to Gamma Ray*, vol. 7011 of *Proceedings of SPIE*, June 2008.

[21] P. C. Agrawal, "A broad spectral band Indian Astronomy satellite 'Astrosat'," *Advances in Space Research*, vol. 38, no. 12, pp. 2989–2994, 2006.

[22] F. E. Christensen, A. Hornstrup, N. J. Westergaard, H. W. Schnopper, J. Wood, and K. Parker, "Graded d-spacing multilayer telescope for high-energy x-ray astronomy," in *Multilayer and Grazing Incidence X-Ray/EUV Optics*, vol. 1546 of *Proceedings of SPIE*, pp. 160–167, San Diego, Calif, USA, July 1991.

[23] K. Yamashita, "Supermirror hard-x-ray telescope," *Applied Optics*, vol. 37, no. 34, pp. 8067–8073, 1998.

[24] F. Berendse, S. M. Owens, P. J. Serlemitsos et al., "Production and performance of the InFOCμS 20-40-keV graded multilayer mirror," *Applied Optics*, vol. 42, no. 10, pp. 1856–1866, 2003.

[25] Y. Ogasaka, K. Tamura, T. Okajima et al., "Development of supermirror hard X-ray telescope and the results of the first InFOCuS flight observation," in *X-ray and Gamma-Ray telescopes and Instruments for Astronomy*, Proceedings of SPIE, pp. 619–630, August 2002.

[26] R. Shibata, Y. Ogasaka, K. Tamura et al., "Upgraded hard X-ray telescope with multilayer supermirror for the InFOCμS balloon experiment," in *UV and Gamma-Ray Space Telescope Systems*, Proceedings of SPIE, pp. 313–324, June 2004.

[27] T. Okajima, K. Tamura, Y. Ogasaka et al., "Characterization of the supermirror hard-x-ray telescope for the InFOCμS balloon experiment," *Applied Optics*, vol. 41, no. 25, pp. 5417–5426, 2002.

[28] R. Shibata, Y. Ogasaka, K. Tamura et al., "Development of hard X-ray telescope for InFOCμS balloon experiment," in *Optics for EUV, X-Ray, and Gamma-Ray Astronomy II*, Proceedings of SPIE, pp. 1–12, August 2005.

[29] T. Miyazawa, R. Shibata, Y. Ogasaka et al., "Development and performance of the advanced hard x-ray telescope for the balloon experiment," in *Space Telescopes and Instrumentation II: Ultraviolet to Gamma Ray*, Proceedings of SPIE, May 2006.

[30] Y. Ogasaka, K. Tamura, T. Miyazawa et al., "Thin-foil multilayer-supermirror hard X-ray telescope for InFOC S/SUMIT balloon exeriments and NeXT satellite program," in *Optics for EUV, X-Ray, and Gamma-Ray Astronomy III*, Proceedings of SPIE, August 2007.

[31] H. Awaki, Y. Ogasaka, H. Kunieda et al., "Current status of the Astro-H X-ray telescope system," in *Optics for EUV, X-Ray, and Gamma-Ray Astronomy IV*, Proceedings of SPIE, August 2009.

[32] H. Kunieda and P. J. Serlemitsos, "X-ray mirror assessment with optical light," *Applied Optics*, vol. 27, no. 8, pp. 1544–1547, 1988.

[33] C. J. Hailey, S. Abdali, F. E. Christensen et al., "Investigation of substrates and mounting techniques for the High Energy Focusing Telescope (HEFT)," in *EUV, X-Ray, and Gamma-Ray Instrumentation for Astronomy VIII*, vol. 3114 of *Proceedings of SPIE*, pp. 535–543, July 1997.

[34] P. H. Mao, F. A. Harrison, Y. Y. Platonov et al., "Development of grazing incidence multilayer mirrors for hard X-ray focusing telescopes," in *EUV, X-Ray, and Gamma-Ray Instrumentation for Astronomy VIII*, vol. 3114 of *Proceedings of SPIE*, pp. 526–534, July 1997.

[35] J. E. Koglin, C. M.H. Chen, J. C. Chonko et al., "Hard X-ray optics: from HEFT to NuSTAR," in *UV and Gamma-Ray Space Telescope Systems*, vol. 5488 of *Proceedings of SPIE*, pp. 856–867, June 2004.

[36] J. E. Koglin, W. H. Baumgartner, C. M. H. Chen et al., "Calibration of heft hard X-ray optics," in *X-Ray Universe 2005*, A. Wilson, Ed., vol. 2 of *ESA SP-604*, pp. 955–960, September 2006.

[37] J. E. Koglin, H. An, K. L. Blaedel et al., "NuSTAR Hard X-ray Optics Design and Performance," in *Optics for EUV, X-Ray, and Gamma-Ray Astronomy IV*, Proceedings of SPIE, August 2009.

[38] M. Bavdaza, PH. Gondoina, K. Wallaceb et al., "IXO system studies and technology preparation," in *Optics for EUV, X-Ray, and Gamma-Ray Astronomy IV*, Proceedings of SPIE, August 2009.

[39] M. J. Collon, R. Günther, M. Ackermann et al., "Stacking of silicon pore optics for IXO," in *Optics for EUV, X-Ray, and Gamma-Ray Astronomy IV*, Proceedings of SPIE, August 2009.

[40] M. Bavdaz, M. Collon, M. Beijersbergen, K. Wallace, and E. Wille, "X-ray pore optics technologies and their application in space telescopes," *X-Ray Optics and Instrumentation*, vol. 2010, Article ID 295095, 15 pages, 2010.

[41] W. W. Zhang, J. Bolognese, G. Byron et al., "Mirror technology development for the international x-ray observatory (IXO) mission," in *EUV and X-Ray Optics: Synergy between Laboratory and Space*, Proceedings of SPIE, April 2009.

[42] M. Vongehr, P. Friedrich, H. Bräuninger et al., "Experimental results on slumped glass x-ray mirror segments," in *Optics for EUV, X-Ray, and Gamma-Ray Astronomy III*, vol. 6688 of *Proceedings of SPIE*, August 2007.

[43] M. Ghigo, S. Basso, R. Canestrari et al., "Hot slumping glass technology and integration process to manufacture a grazing incidence scaled prototype for the ixo telescope modules," in *Optics for EUV, X-Ray, and Gamma-Ray Astronomy IV*, vol. 7437 of *Proceedings of SPIE*, August 2009.

[44] R. S. Mcclelland, T. M. Carnahan, M. K. Choi, D. W. Robinson, and T. T. Saha, "Preliminary design of the international X-ray observatory flight mirror assembly," in *Optics for EUV, X-Ray, and Gamma-Ray Astronomy IV*, Proceedings of SPIE, August 2009.

[45] W. W. Zhang, J. Bolognese, G. Byron et al., "Constellation-X mirror technology development," in *Space Telescopes and Instrumentation 2008: Ultraviolet to Gamma Ray*, Proceedings of SPIE, June 2008.

[46] F. E. Christensen, C. P. Jensen, K. K. Madsen et al., "Novel multilayer designs for future hard X-ray missions," in *Space Telescopes and Instrumentation II: Ultraviolet to Gamma Ray*, Proceedings of SPIE, May 2006.

[47] C. P. Jensen, F. E. Christensen, S. Romaine, R. Bruni, and Z. Zhong, "Stacked depth graded multilayer for hard X-rays, measured up to 130 keV," in *Optics for EUV, X-Ray, and Gamma-Ray Astronomy III*, Proceedings of SPIE, August 2007.

[48] S. J. Wolk, R. J. Brissenden, M. Elvis et al., "Science with generation-X," in *Space Telescopes and Instrumentation 2008: Ultraviolet to Gamma Ray*, Proceedings of SPIE, June 2008.

[49] D. A. Schwartz, R. J. Brissenden, M. Elvis et al., "On-orbit adjustment calculation for the Generation-X X-ray mirror figure," in *Space Telescopes and Instrumentation 2008: Ultraviolet to Gamma Ray*, Proceedings of SPIE, June 2008.